Journal of
Mechanics of
Materials and Structures

EDGE FLUTTER OF LONG BEAMS UNDER FOLLOWER LOADS

Emmanuel de Langre and Olivier Doaré

Volume 10, No. 3 May 2015

msp

JOURNAL OF MECHANICS OF MATERIALS AND STRUCTURES
Vol. 10, No. 3, 2015
dx.doi.org/10.2140/jomms.2015.10.283

msp

EDGE FLUTTER OF LONG BEAMS UNDER FOLLOWER LOADS

EMMANUEL DE LANGRE AND OLIVIER DOARÉ

The linear instability of a beam tensioned by its own weight is considered. It is shown that for long beams, in the sense of an adequate dimensionless parameter, the characteristics of the instability caused by a follower force do not depend on the length. The asymptotic regime significantly differs from that of short beams: flutter prevails for all types of follower loads, and flutter is localised at the edge of the beam. An approximate solution using matched asymptotic expansion is proposed for the case of a semi-infinite beam. Using a local criterion based on the stability of waves, the characteristics of this regime as well as its range of application can be well predicted. These results are finally discussed in relation with cases of flow-induced instabilities of slender structures.

1. Introduction

The linear stability of a beam under the action of a follower force exerted at one of its extremities has been the subject of intensive research, as can be seen from the extensive review in [Langthjem and Sugiyama 2000]. The interest in this problem lies in its potential applications and also in the large variety of fundamental topics of mechanics involved in the solution method. Practical examples of direct application in the field of fluid-structure interactions are numerous: fluid-conveying pipes, plates subjected to axial flow and towed cylindrical bodies are modelled by equations that are similar, though not identical, to those of a beam under a compressive follower force [Païdoussis 1998; 2003]. More generally, follower forces have been extensively discussed in the literature, including in terms of their physical reality; see [Elishakoff 2005] for a full review. The case of a cantilevered beam of finite length under a partial follower force is well documented [Bolotin 1963], with many results on the effect of characteristics of the beam or of the load on the critical load that causes instability, and on the nature of the instability, be it divergence (buckling) or flutter.

We seek here to establish the characteristics of instability of a beam in the case where its length is much larger than the region where an unstable motion will develop. This arises when a constant load, such as gravity acting on a vertically hanging beam, produces a tension that increases along the beam, from zero at the lower free end to a maximum at the upper fixed end. The increasing tension induces a corresponding increasing stiffness. Motion is then confined to the lower end, corresponding to *edge flutter*. This has been studied both experimentally and numerically in three of the problems of flow-induced vibrations mentioned above: hanging fluid-conveying pipes [de Langre et al. 2001; Doaré and de Langre 2002], hanging ribbons under axial flow [Lemaitre et al. 2005] and towed cylinders under axial flow [de Langre et al. 2007; Obligado and Bourgoin 2013]. In all these systems it was observed that there exists a limit state in which the length does not affect the stability. This limit state is found for

Keywords: follower force, flutter instability, semi-infinite, matched asymptotic expansion.

length larger than a limit value given by simple considerations on the local stability of bending waves [Doaré and de Langre 2002; de Langre et al. 2007].

The objective of this paper is to establish similar results in the generic case of a beam under a partial follower force (or subtangential force), tensioned by a load such as gravity.

In Section 2 we shall recall the equations of motion and the possible choices of dimensionless variables. The effect of the beam length on stability is analysed in Section 3, using numerical computations of the eigenmodes. In Section 4 we address the particular case of a semi-infinite beam, using various types of modelling. The application of the results given in the paper to problems of flow-induced instabilities is discussed in Section 5.

2. Equations of motion

We consider a vertical beam of length L loaded by its own weight; see Figure 1.

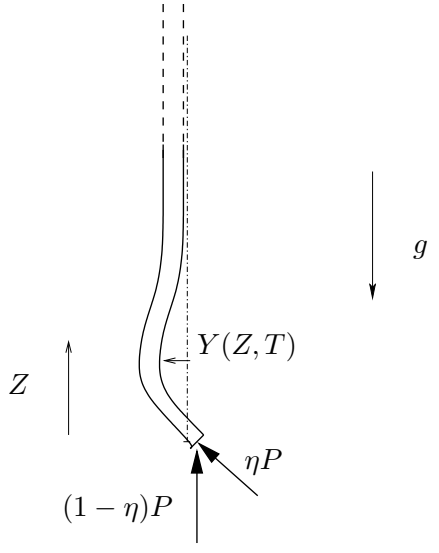

Figure 1. Semi-infinite hanging beam with a partial follower force.

A partial follower force is applied at its lower end [Langthjem and Sugiyama 2000]. The linear equation governing the in-plane lateral deflection $Y(Z, T)$ reads

$$EI\frac{\partial^4 Y}{\partial Z^4} + \frac{\partial}{\partial Z}\left[(P - mgZ)\frac{\partial Y}{\partial Z}\right] + m\frac{\partial^2 Y}{\partial T^2} = 0, \tag{1}$$

where EI is the flexural rigidity, P is the load, g is gravity and m is the mass per unit length. No damping is considered here, though it is known to significantly influence some aspects of the problem; see, for instance, [Detinko 2003]. The boundary conditions at the lower end, $Z = 0$, are

$$EI\frac{\partial^2 Y}{\partial Z^2}(0) = 0, \quad EI\frac{\partial^3 Y}{\partial Z^3}(0) + (1-\eta)P\frac{\partial Y}{\partial Z}(0) = 0, \tag{2}$$

where η is a coefficient that expresses the part of the loading that follows the beam slope; $\eta = 0$ corresponds to a nonfollower force and $\eta = 1$ to a pure follower force. At the upper end, we assume a clamped condition,

$$Y(L) = 0, \quad \frac{\partial Y}{\partial Z}(L) = 0. \tag{3}$$

Using the length of the beam, L, as a reference, we define the dimensionless variables

$$z = \frac{Z}{L}, \quad y = \frac{Y}{L}, \quad t = \left(\frac{EI}{m}\right)^{1/2} \frac{1}{L^2} T, \quad p = \frac{PL^2}{EI}, \quad \gamma = \frac{mgL^3}{EI}. \tag{4}$$

Then (1) may be rewritten in dimensionless form as

$$\frac{\partial^4 y}{\partial z^4} + \frac{\partial}{\partial z}\left[(p - \gamma z)\frac{\partial y}{\partial z}\right] + \frac{\partial^2 y}{\partial t^2} = 0, \tag{5}$$

with the boundary conditions

$$\frac{\partial^2 y}{\partial z^2}(0) = 0, \quad \frac{\partial^3 y}{\partial z^3}(0) + (1 - \eta) p \frac{\partial y}{\partial z}(0) = 0, \quad y(1) = 0, \quad \frac{\partial y}{\partial z}(1) = 0. \tag{6}$$

This dimensionless set of equations is adequate to analyse the effect of γ on the critical loading, but only if the length L is kept constant. As we need to vary the length L, it is necessary to define a new set of dimensionless parameters. We now use a length scale defined by the ratio of the two stiffnesses of the beam, namely the flexural rigidity and the stiffness related to tension induced by gravity [Doaré and de Langre 2002],

$$L_g = \left(\frac{EI}{mg}\right)^{1/3}, \tag{7}$$

which will be referred to as the gravity length. This length scales like the critical length that causes buckling of the beam under its own weight. Using L_g as the reference length to define dimensionless variables, we have

$$x = \frac{Z}{L_g}, \quad y = \frac{Y}{L_g}, \quad \tau = \left(\frac{EI}{m}\right)^{1/2} \frac{1}{L_g^2} T, \quad q = \frac{PL_g^2}{EI}, \quad \ell = \frac{L}{L_g}, \tag{8}$$

where L_g has been substituted for L. These are related to the previous set of variables by

$$x = z\ell, \quad \tau = t\ell^2, \quad q = \frac{p}{\ell^2}, \quad \ell = \gamma^{1/3}. \tag{9}$$

Equation (1) now becomes

$$\frac{\partial^4 y}{\partial x^4} + \frac{\partial}{\partial x}\left[(q - x)\frac{\partial y}{\partial x}\right] + \frac{\partial^2 y}{\partial \tau^2} = 0, \tag{10}$$

and the corresponding boundary conditions are

$$\frac{\partial^2 y}{\partial x^2}(0) = 0, \quad \frac{\partial^3 y}{\partial x^3}(0) + (1 - \eta) q \frac{\partial y}{\partial x}(0) = 0, \quad y(\ell) = 0, \quad \frac{\partial y}{\partial x}(\ell) = 0. \tag{11}$$

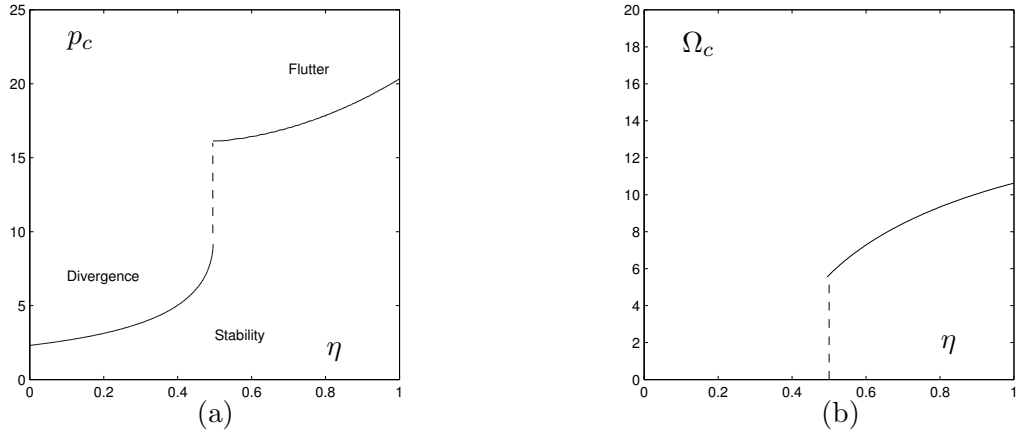

Figure 2. (a) Critical load and (b) frequency at instability, for short beams. Dashed vertical lines are guides for the eyes that do not correspond to calculations.

3. Stability of finite beams

3.1. ***Solution for short beams.*** For short beams, in the sense that $\ell \ll 1$, the critical load q_c may be derived by considering that $\gamma \ll 1$, so that (5) becomes

$$\frac{\partial^4 y}{\partial z} + p\frac{\partial^2 y}{\partial z^2} + \frac{\partial^2 y}{\partial t^2} = 0. \tag{12}$$

The corresponding stability diagram of p_c versus η is that of the generalised Beck's column [Langthjem and Sugiyama 2000], and is shown in Figure 2(a). For $\eta < 0.5$, instability arises in the form of a divergence, whereas flutter prevails for $\eta > 0.5$. The corresponding frequency at the flutter limit is shown in Figure 2(b). The critical load and frequency at flutter expressed in the dimensionless variables of (8) are

$$q_c(\eta, \ell) = \frac{p_c(\eta)}{\ell^2}, \quad \omega_c(\eta, \ell) = \frac{\Omega_c(\eta)}{\ell^2}. \tag{13}$$

3.2. ***Effect of length.*** We now investigate the effect of the length ℓ on the stability threshold and the nature of the instability. The numerical method utilised to this end is the finite difference method, as in [Sugiyama and Kawagoe 1975]. It allows us to compute the eigenvalues ω and the eigenvectors φ, such that

$$\varphi^{(4)} + [(q - x)\varphi']' - \omega^2\varphi = 0 \tag{14}$$

with

$$\varphi''(0) = \varphi^{(3)}(0) + (1 - \eta)q\varphi'(0) = \varphi(\ell) = \varphi'(\ell) = 0. \tag{15}$$

The critical load and the nature of the corresponding instability can be determined from the evolution of the real and imaginary parts of the frequency. The beam is unstable if the frequency ω has a negative imaginary part. If the real part is zero, the instability results in an exponential growth in time of the deformation, without oscillation, and the instability is of the divergence type. If the real part is nonzero, the instability results in an exponential growth of oscillations, and the instability is of the flutter type.

Figure 3 shows the evolution of the critical load with length, for several values of η of particular interest.

For $\eta = 0$, Figure 3(a), which is the case of a nonfollower force, the critical load decreases steeply with length up to about $\ell = 5$, where it reaches a limit value and does not change when the length is increased further. Instability is of the divergence type for all lengths. In the same figure are shown computations from [Naguleswaran 2004; Triantafyllou and Chryssostomidis 1984] for intermediate values of the length. In [Triantafyllou and Chryssostomidis 1984], the static instability of a towed beam is considered, which yields equations similar to those used here. Details of the equivalence are discussed in Section 5, but suffice it to say here that we may use the results in Figure 4 of [Triantafyllou and Chryssostomidis 1984] with the change of variables $\ell = \varepsilon\lambda^{2/3}$ and $q = \lambda^{2/3}$. It is seen that those results and those of this paper are in very good agreement. For $\eta = 0.2$, Figure 3(b), the critical load for divergence also decreases and reaches a limit value, but the flutter threshold becomes lower than that for divergence for beams longer than $\ell = 5$. For $\eta = 0.3$, Figure 3(c), no divergence is found for $\ell > 3$. Instability in that range of ℓ is of the flutter type. For $\eta = 1$, Figure 3(d), the system loses stability by flutter, similarly to Beck's column; the critical load for flutter decreases with ℓ until it reaches a limit value.

From these four cases it can be stated that there exists a limit configuration for all long beams, say $\ell > 10$. For these lengths, the type of instability, flutter or divergence, may differ from that observed for short beams at the same value of η.

This is further confirmed in the evolutions of the stability diagram $q_c(\eta)$ shown in Figure 4. At $\ell = 1$, the diagram is similar, though not identical, to that for short beams; since $\ell = 1$, we have here $q_c = p_c$, and Figures 2 and 4(a) can be directly compared. At $\ell = 100$, Figure 4(b), a limit state is almost reached, where stability is always lost by flutter, for all values of η.

Figure 5 shows the mode shape at the critical load, which may be a divergence or a flutter instability depending on the values of η and ℓ, as shown above. Note that at the instability threshold φ is real, even for flutter instability. In fact, in (14), when ω is real, so is φ. For $\eta = 0$, Figure 5(a), the mode shape, here for divergence, becomes independent of the length when $\ell > 3$. This is consistent with Figure 3(a), where the critical load was found to be stationary in this range. For $\eta = 0.3$ and $\eta = 1$, Figures 5(b) and (c), the mode shapes also converge to a constant shape as the length is increased. There, the displacement is confined to the lower part of the beam. Note that the instability is of the flutter type, except for $\eta = 0.3$ at $\ell = 1$. Yet the limit mode shape closely resembles that of the divergence instability at $\eta = 0$.

4. Stability of a semi-infinite beam

4.1. ***Boundary conditions.*** We now seek to determine the characteristics of the instability when the beam is assumed to be of infinite length in the X axis. This is expected to be the solution to which the results of the preceding section converge as ℓ is increased. Whereas the boundary condition at the lower end is unchanged, the condition that the beam is clamped at $X = L$ needs to be replaced by the conditions that the displacement remains finite as X goes to infinity and that in this limit, propagating waves only radiate in the direction of increasing X. These conditions, in dimensionless form, read

$$\lim_{x\to\infty} |y| = 0 \qquad \lim_{x\to\infty} \frac{\partial y}{\partial x}\frac{\partial y}{\partial t} < 0. \tag{16}$$

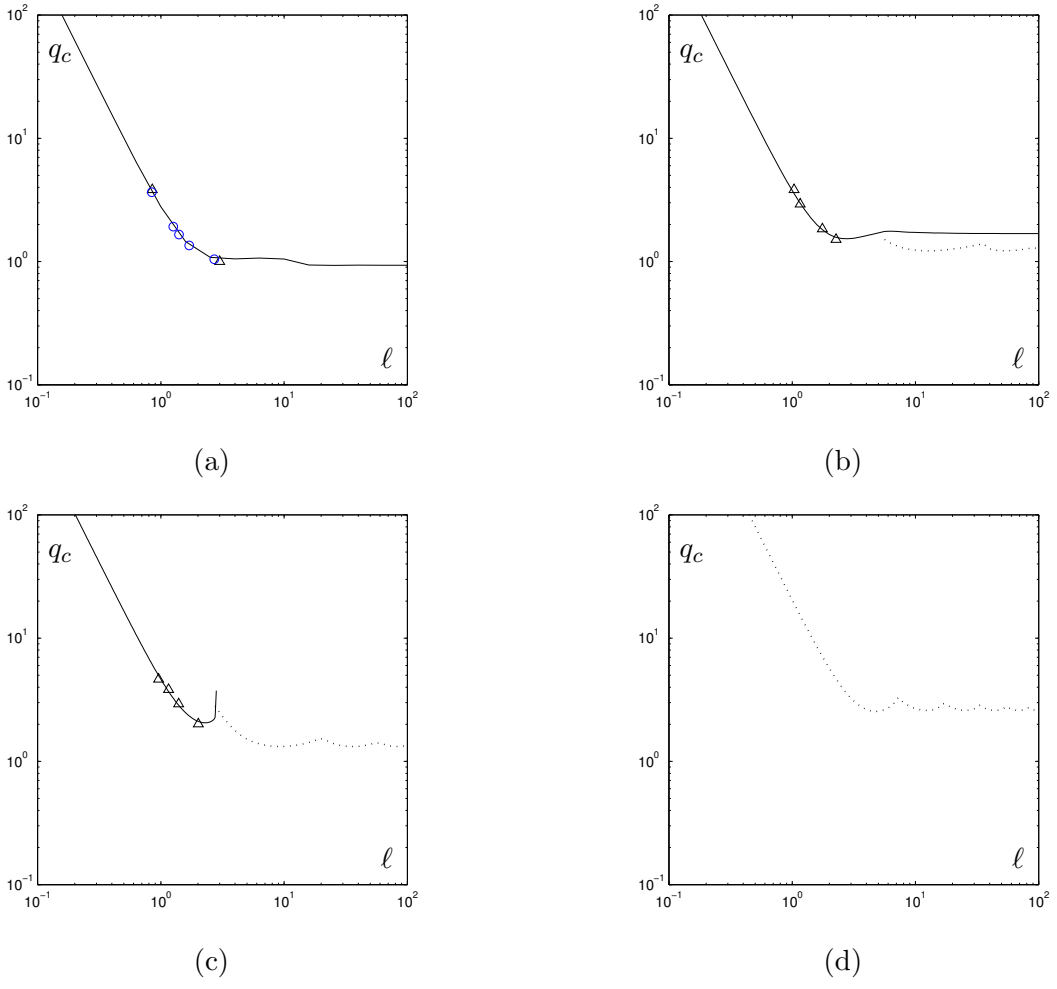

Figure 3. Effect of length on the critical load for divergence and flutter instabilities: (a) $\eta = 0$, (b) $\eta = 0.2$, (c) $\eta = 0.3$, (d) $\eta = 1$. The notation (—) represents results for divergence; $(\cdots)$, results for flutter; $(\circ)$, computations by [Naguleswaran 2004]; (Δ), computations by [Triantafyllou and Chryssostomidis 1984].

4.2. ***Divergence instability.*** The case of divergence instability may be analysed by neglecting all time derivatives in the equations, so that (10) becomes

$$\frac{\partial^4 y}{\partial x^4} + \frac{\partial}{\partial x}\left[(q - x)\frac{\partial y}{\partial x}\right] = 0 \tag{17}$$

and the boundary conditions are only

$$\frac{\partial^2 y}{\partial x^2}(0) = 0, \quad \frac{\partial^3 y}{\partial x^3}(0) + (1 - \eta)q\frac{\partial y}{\partial x}(0) = 0, \quad \lim_{x\to\infty} |y| = 0. \tag{18}$$

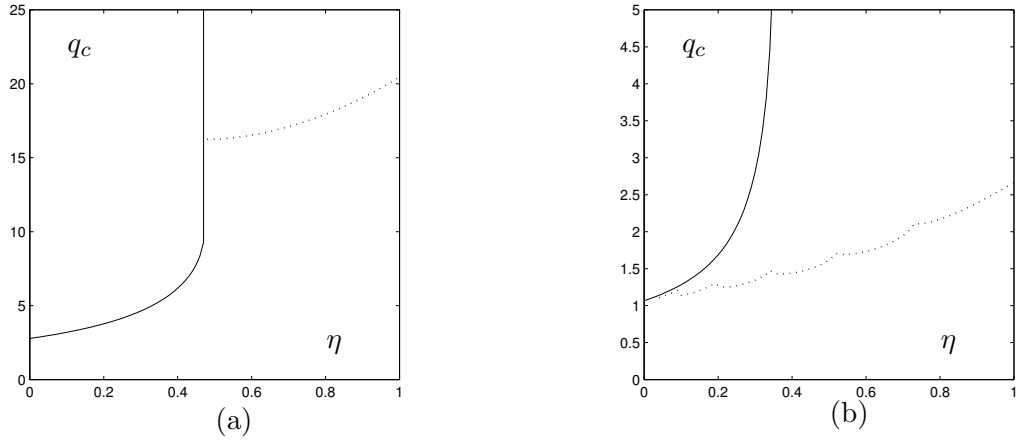

Figure 4. Effect of the ratio η on the critical load for divergence (—) and flutter $(\cdots)$. (a) Short beam, $\ell = 1$, (b) long beam, $\ell = 100$.

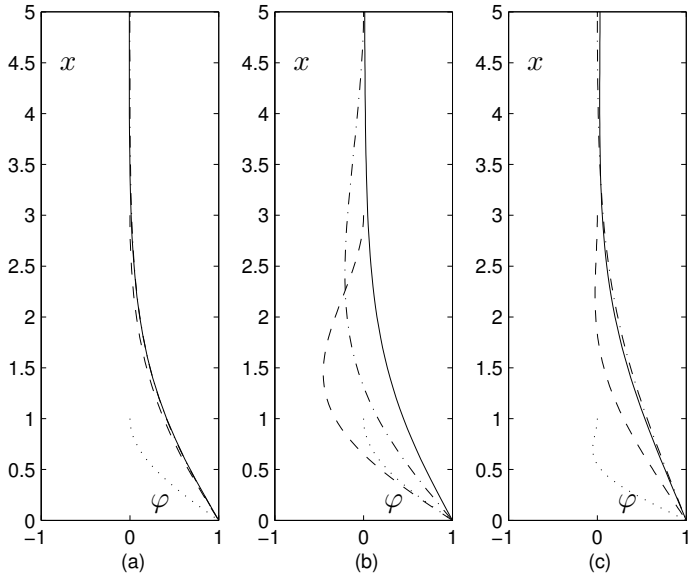

Figure 5. Mode shape at the critical load. (a) $\eta = 0$, (b) $\eta = 0.3$, (c) $\eta = 1$. $(\cdots)$, $\ell = 1$; $(--)$, $\ell = 3$; $(-\cdot-)$, $\ell = 5$; (—), $\ell = 10$.

By defining $\lambda = q^{3/2}$ and $Z = x - q$, this set of equations is identical to that solved by Triantafyllou and Chryssostomidis [1984] for the case of a towed cylinder. Using their solution with our variables, the critical load for divergence $q_c(\eta)$ is found to satisfy

$$\mathrm{Ai}'(-q_c) - q_c\eta\left[\frac{1}{3} - \int_0^{-q_c} \mathrm{Ai}(s)\,ds\right] = 0, \tag{19}$$

where Ai is the Airy function [Abramowitz and Stegun 1972].

4.3. ***Flutter instability.*** We give here an approximate solution for the critical load for flutter of a semi-infinite beam, which is an extension of [de Langre et al. 2001] for a purely follower force, $\eta = 1$. The approach used in the matched asymptotic expansions follows that proposed in [Triantafyllou and Triantafyllou 1991] for the dynamics of vibrating strings tensioned by gravity.

We consider (10), with the boundary conditions (11) at the bottom end and (16) for a semi-infinite beam. We seek harmonic solutions of this set of equations, of the form

$$y(x,t) = \text{Real}[\varphi(x)e^{i\omega t}] \tag{20}$$

as a function of the follower force magnitude q. Instability will be associated with $\text{Im}(\omega) < 0$. The variation in space of the solution satisfies

$$\varphi^{(4)} + [(q-x)\varphi']' - \omega^2\varphi = 0, \tag{21}$$

with boundary conditions

$$\varphi^{(2)}(0) = 0, \quad \varphi^{(3)}(0) + (1-\eta)q\varphi'(0) = 0, \tag{22}$$

where the prime denotes derivation with respect to x. The condition for radiating waves reads

$$\lim_{x\to\infty} \left(\text{Real}[\varphi'(x)e^{i\omega t}]\,\text{Real}[i\omega\varphi(x)e^{i\omega t}]\right) < 0. \tag{23}$$

Let us consider first the lower part of the beam, where x is of the order of q. In this "inner" domain of length q, we may derive an approximate solution $\varphi_i(x)$ by simply lumping all its inertia at the lower end of the beam, so that the boundary conditions at $x = 0$ read now

$$\varphi_i^{(2)}(0) = 0, \quad \varphi_i^{(3)}(0) + (1-\eta)q\varphi_i'(0) = q\omega^2\varphi_i(0), \tag{24}$$

and (21) reduces to

$$\varphi_i^{(4)} + [(q-x)\varphi_i']' = 0. \tag{25}$$

The corresponding solution reads

$$\varphi_i(x) = a + \int_0^x \left[b\,\text{Ai}(s-q) + c\,\text{Bi}(s-q) + d\,\text{Gi}(s-q)\right] ds, \tag{26}$$

where Ai, Bi and Gi are the Airy functions, a, b, c, d being four coefficients. For the sake of clarity, we now use the notation $\overline{F}(x) = \int_0^x F(s)\,ds$ and F for $F(-q)$ unless otherwise specified, where F could be any of the Airy functions above.

In terms of the coefficients a, b, c, d, the boundary conditions at the lower end are

$$b\,\text{Ai}' + c\,\text{Bi}' + d\,\text{Gi}' = 0, \tag{27}$$

$$b\,\text{Ai}'' + c\,\text{Bi}'' + d\,\text{Gi}'' + (1-\eta)q(b\,\text{Ai} + c\,\text{Bi} + d\,\text{Gi}) = aq\omega^2. \tag{28}$$

Conversely, in the upper part of the beam, that is, where $x \gg q$, we rescale the equations by using new variables in space and time, namely

$$\chi = x\varepsilon, \quad r = \frac{\omega}{\sqrt{\varepsilon}}, \tag{29}$$

where $\varepsilon = L_g/\Lambda$, the length Λ being an arbitrary large length scale. Using this set of variables, (21) reads

$$\varepsilon^3\varphi^{(4)} + [(\varepsilon^2 q - \varepsilon\chi)\varphi']' - \varepsilon r^2\varphi = 0, \tag{30}$$

where the prime now denotes differentiation with respect to χ. This allows us to derive the equation at the leading order in the "outer" domain,

$$(-\chi\varphi_e')' - r^2\varphi_e = 0, \tag{31}$$

the solution of which, in terms of Bessel functions, is (see also in [Elishakoff and Pellegrini 1987])

$$\varphi_e(\chi) = \alpha J_0(2r\sqrt{\chi}) + \beta Y_0(2r\sqrt{\chi}). \tag{32}$$

The radiation condition, (23), implies that

$$\alpha - i\beta = 0. \tag{33}$$

We may now match the inner and outer solutions by considering their respective limits [Abramowitz and Stegun 1972; Triantafyllou and Triantafyllou 1991]. Equating these two limits yields three conditions for the coefficients defining the inner and outer solutions, namely

$$c = 0, \quad d = \beta, \quad a + b\left[\frac{1}{3} - \overline{\mathrm{Ai}}\right] + d\left[\frac{2\gamma + \ln 3}{3\pi} - \overline{\mathrm{Gi}}\right] = \alpha + \beta\frac{2}{\pi}(\ln\omega + \gamma), \tag{34}$$

where γ is Euler's constant. The set of boundary conditions (27), (28), (33), with the three matching conditions (34), are six linear equations between the six coefficients α, β, a, b, c, d. This defines an implicit relationship between the two parameters ω and q, so that there exists a nontrivial solution

$$-\eta q[\mathrm{Gi}'\,\mathrm{Ai} - \mathrm{Gi}\,\mathrm{Ai}'] - \frac{1}{\pi}\,\mathrm{Ai}' + q\omega^2\left[\left(\frac{1}{3} - \overline{\mathrm{Ai}}\right)\mathrm{Gi}' - \left(\frac{\ln 3 - 4\gamma - 3i\pi - 6\ln\omega}{3\pi} - \overline{\mathrm{Gi}}\right)\mathrm{Ai}'\right] = 0. \tag{35}$$

The particular value of the flutter instability threshold q_c may be directly derived by assuming that ω is real in (35). As all functions of q in (35) are real, this implies that

$$\mathrm{Ai}'(-q_c) = 0, \quad q_c \simeq 1.02. \tag{36}$$

The real part of the frequency at the instability threshold is then derived using (35) and (36) as

$$\omega_c^2 = \eta\frac{\mathrm{Ai}(-q_c)}{\frac{1}{3} - \overline{\mathrm{Ai}}(-q_c)}. \tag{37}$$

At $\eta = 0$, the solution of [Triantafyllou and Chryssostomidis 1984] for divergence is recovered, both in terms of critical load and frequency. Using this approximate solution, flutter is found to exist for all values of η, and the corresponding critical load does not vary with η. In Figure 6(a) this is compared with the numerical solution for very long beams, $\ell = 100$. The approximate solution, (36), predicts a lower bound, $q_c = 10.2$, equal to that for $\eta = 0$. The flutter frequency is very well predicted, as may be seen in Figure 6(b). At the instability threshold, the modal shape φ is real and reduces to

$$\varphi(x) = \int_0^x \mathrm{Ai}(s - p)\,ds - \tfrac{1}{3}. \tag{38}$$

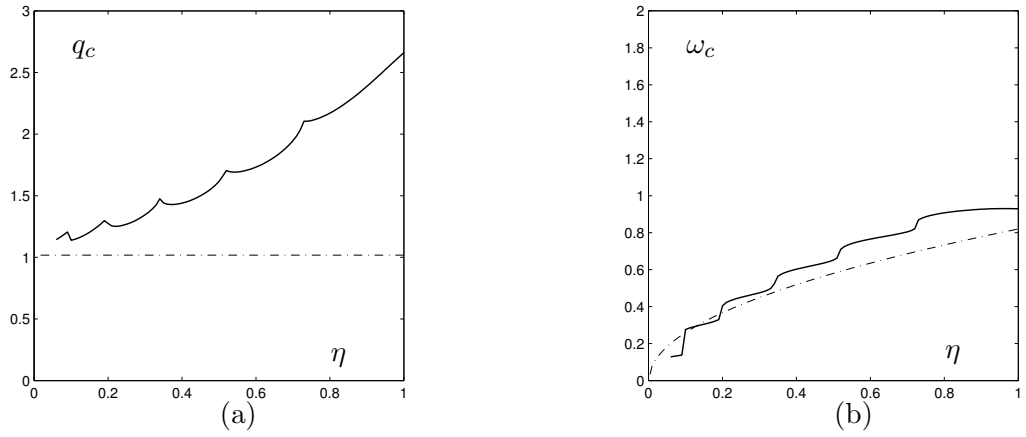

Figure 6. (a) Critical load q_c and (b) frequency ω_c of flutter of a long beam. (—), numerical results for $\ell = 100$; $(- \cdot -)$ solution for the semi-infinite beam using matched asymptotic expansions; see (36) and (37).

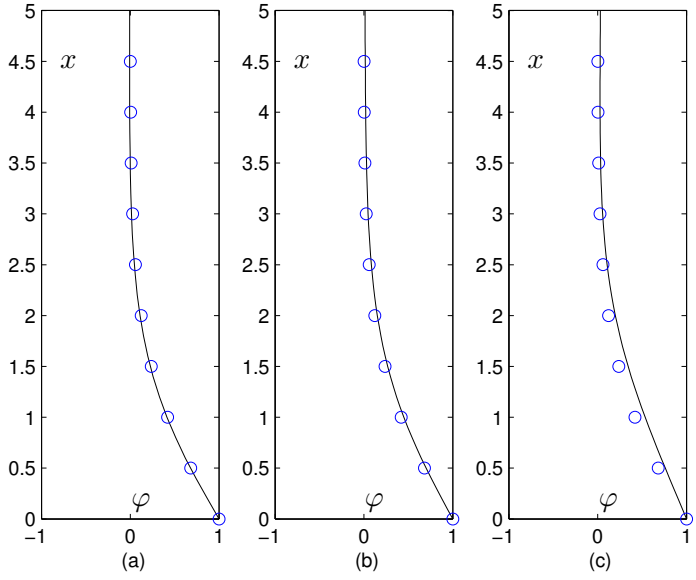

Figure 7. Mode shape at the critical load for a long beam. (a) $\eta = 0$, (b) $\eta = 0.3$, (c) $\eta = 1$. (—), numerical results for $\ell = 10$; (○), solution for the semi-infinite beam using matched asymptotic expansions; see Equation (38).

This is compared in Figure 7 with the computed mode shapes at $\ell = 10$. For $\eta = 0$, Figure 7(a), (38) is actually the exact solution for a semi-infinite beam, which derives from the results of [Triantafyllou and Chryssostomidis 1984]. For $\eta = 0.3$ and even $\eta = 1$, it is remarkable that (38) stills gives a very good approximation of the mode shape at the flutter threshold; see Figures 7(b) and (c).

4.4. ***A model based on local wave stability.*** Following [Doaré and de Langre 2002], we consider now a criterion based on the local characteristics of waves, at a given position x. From (10), the dispersion relation is

$$k^4 - (q - x)k^2 - \omega^2 = 0, \tag{39}$$

where k is the wavenumber and ω is the frequency of the wave. All points such that $x < q$ bear unstable waves. Beams of length ℓ larger than q are expected to have a behaviour not affected by length, as waves are damped above $x = q$.

In dimensional variables, this allows us to define the length L_N for neutral stability,

$$L_N = \frac{P}{mg}, \tag{40}$$

above which the medium only bears stable waves. In (1) this is the point where the local tension goes through zero. Considering that the part of the beam above this, $Z > L_N$, plays a negligible role in the instability, we may approximate the critical load for the *semi-infinite* beam by that for a *finite* beam of length L_N: a beam of length L_N, without gravity, has a dimensional critical load

$$P_c = \frac{EI}{L_N^2} p_c, \tag{41}$$

where p_c is the dimensionless critical load for short beams. As the length L_N varies with the load P, this results in

$$P_c^3 = EI\,(mg)^2 p_c. \tag{42}$$

Using now dimensionless variables pertaining to the case of long beams, this reads

$$q_c = p_c^{1/3}; \tag{43}$$

similarly, we have

$$\omega_c = \frac{\Omega_c}{p_c^{2/3}}. \tag{44}$$

In Figure 8(a), this is plotted for comparison with numerical results for the very long beam. The order of magnitude of the critical load is well recovered. Yet divergence is predicted for $\eta < 0.5$, instead of flutter. Note also that the critical load at $\eta = 1$ is very well predicted. Figure 8(b) summarises this approach: the limit line $\ell = q$ is found to be a good approximation of the transition between the behaviour of short beams, which depends on length, and that of long beams, which does not. For short beams, the approximation (13) applies. For long beams, (43) is a good approximation.

5. Discussion

5.1. ***Domains of instability.*** In the results presented in this paper, two regions can be identified in a beam tensioned by a load such as gravity. In the part near the free end, $x \ll 1$ in our dimensionless variables, that is, $Z \ll L_g = (EI/Mg)^{1/3}$, the stiffness that opposes lateral displacement is dominantly that of the flexural rigidity. Conversely, for $x \gg 1$, the stiffness is due to the tension that results from gravity.

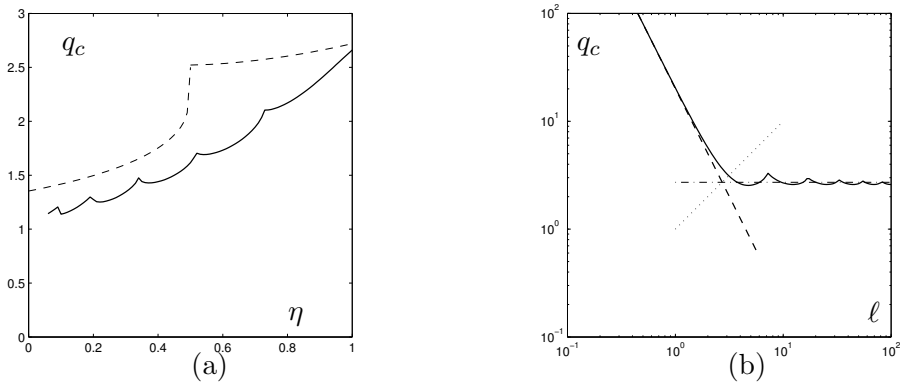

Figure 8. Models for the critical load based on local wave stability. (a) Critical load numerical results (—) for $\ell = 100$; $(- \ -)$, model based on local wave stability; see (43) and (44). (b) Effect of length $\eta = 1$. (—), computations of Section 3.2; $(- \ -)$, short beam model; $(\cdots)$, transition line; $(- \cdot -)$, long beam model.

For a given beam, if its length L is much smaller than L_g, or $\ell \ll 1$, gravity effects can be neglected everywhere. In terms of stability the behaviour is that of short beams in our denomination. The upper boundary condition, here clamping, plays a crucial role, and the instability may be divergence or flutter. If the length is much larger than L_g, so that $\ell \gg 1$, gravity effects dominate in all the upper part. This results in a confinement of the instability in the lower part of the beam, which appears in all the mode shapes. The upper boundary condition plays a lesser role. It is remarkable that the characteristics of the instability of these long beams seem to be much simpler than that of short beams: flutter prevails in all cases, and the critical load, the frequency and the mode shape have very simple evolutions.

For long beams flutter is reached when the load q is of order 1. In that range of loading, the neutral point where tension vanishes, at $x = q$, is located near the limit between the two regions, $x = 1$. The critical load is then such that, in dimensionless variables,

$$P \simeq (EI)^{1/3}(mg)^{2/3}, \tag{45}$$

which shows the balance between the loading P and the two stiffnesses of the systems, EI for the flexural rigidity and mg for the tension induced by gravity.

It should be recalled here that damping was not considered in our calculations. Damping may significantly modify the critical value for flutter instability even when small [Langthjem and Sugiyama 2000], and has been found to have both stabilising and destabilising effects. In some cases, such as that of Beck's column, it has been found that addition of damping destabilises the system and changes the instability type from flutter to buckling. In gyroscopic systems such as fluid-conveying pipes or plates in axial flows, damping was found to destabilise neutral waves at zero frequency [Doaré 2010; 2014], which may also cause the instability to change from flutter to buckling in finite length systems. The generalisation to the present case of a semi-infinite system tensioned by gravity needs to be addressed to see how damping could alter the buckling/flutter stability maps, and if it prevents flutter from prevailing for all values of the follower force coefficient η.

5.2. ***Relation to flow-induced instabilities.*** The equivalence between the loading produced by the flow along a structure and a follower force exerted at its free end is discussed in [Païdoussis 1998; 2003]. Depending on the geometry of the problem, the load may be either a fully follower load (fluid-conveying pipe) or partially a follower load (cylinder with axial flow). In the latter case, the shape of the downstream free end strongly influences the value of η.

For systems mainly tensioned by gravity, such as hanging fluid-conveying pipes or hanging ribbons under axial flow [Doaré and de Langre 2002; Lemaitre et al. 2005], the equations of motion can be put in the common dimensionless form

$$\frac{\partial^4 y}{\partial x^4} + \frac{\partial}{\partial x}\left[(v^2 - x)\frac{\partial y}{\partial x}\right] + 2v\sqrt{\beta}\frac{\partial^2 y}{\partial x \partial \tau} + \frac{\partial^2 y}{\partial \tau^2} = 0, \tag{46}$$

where the dimensionless variables have been defined using the length L_g, as we did in the present paper. Here v is a dimensionless flow velocity and β expresses the proportion of the fluid mass in the total mass. The boundary conditions at the lower end read

$$\frac{\partial^2 y}{\partial x^2}(0) = 0, \quad \frac{\partial^3 y}{\partial x^3}(0) = 0, \tag{47}$$

which expresses the case of a purely follower load. Equation (46) is identical to (10), except for the gyroscopic term which is dependent on β. The stability diagram for the case of a long hanging pipe was analysed in [Doaré and de Langre 2002] and for long hanging ribbons in [Lemaitre et al. 2005]. The critical velocity v_c was found to depend on the length in a manner very similar to that found in this paper. For very long pipes, flutter arises at a critical velocity v_c that depends only on β. Defining $q_c = v^2$, and in the particular limit of $\beta = 0$, the results of [Doaré and de Langre 2002] should converge to those found in this paper for $\eta = 1$. This is not exactly the case when the results of [Doaré and de Langre 2002] are used, as there calculations have been done for small but nonvanishing values of β. It is a well known feature that the case $\beta = 0$ is only found as the limit of very small values (10^{-3}) of β [Païdoussis 1998].

If the tensioning load is not gravity but a flow-induced friction on the slender structure, the form of the problem is changed in several ways [Païdoussis 2003]. First, the tensioning load increases with the flow velocity, which does not allow one to define an equivalent to the length L_g, as for gravity. The reference length that can then be defined scales the flow-induced forces that are proportional to volume (added stiffness forces) and those that are proportional to surface area (friction). Second, the friction load is not constant in direction, as is gravity, but acts tangentially to the instantaneous position of the beam. Third, in the case of axial flow outside of a structure, the flow may also induce forces perpendicular to the instantaneous position of the beam, in the form of a transverse drag. Moreover, the boundary condition at the free end includes other terms that depend on the local geometry of the flow. If all time-dependent terms are neglected, to determine the static stability of the beam under flow, the equation defining the deflection reads [Triantafyllou and Chryssostomidis 1984]

$$\frac{\partial^4 y}{\partial s^4} + v^2 \frac{\partial}{\partial s}\left[(1 - s)\frac{\partial y}{\partial s}\right] = 0. \tag{48}$$

Upon defining $x = v^{2/3}s$ and $q = v^{2/3}$, the equation for the static behaviour of the beam, (17), is recovered. If the end condition sustains a force only in the beam axis, as in [Naguleswaran 2004], the results at $\eta = 0$ are recovered. For the analysis of dynamic instability, not only inertial terms need to be considered, as in the case of this paper. A gyroscopic term, as in (46), and a damping term appear, further complicating the behaviour of the system. In the analysis of a long towed cylinder edge flutter was also found [de Langre et al. 2007], confirming the generality of the results presented here in a generic case.

References

[Abramowitz and Stegun 1972] M. Abramowitz and I. A. Stegun (editors), *Handbook of mathematical functions: with formulas, graphs, and mathematical tables*, vol. 55, 10th ed., Wiley, New York, 1972.

[Bolotin 1963] V. V. Bolotin, *Nonconservative problems of the theory of elastic stability*, Macmillan, New York, 1963.

[Detinko 2003] F. M. Detinko, "Lumped damping and stability of Beck column with a tip mass", *Int. J. Solids Struct.* **40**:17 (2003), 4479–4486.

[Doaré 2010] O. Doaré, "Dissipation effect on local and global stability of fluid-conveying pipes", *J. Sound Vib.* **329**:1 (2010), 72–83.

[Doaré 2014] O. Doaré, "Dissipation effect on local and global fluid-elastic instabilities", pp. 67–84 in *Nonlinear physical systems: spectral analysis, stability and bifurcations*, edited by O. N. Kirillov and D. E. Pelinovsky, Wiley, Hoboken, NJ, 2014.

[Doaré and de Langre 2002] O. Doaré and E. de Langre, "Local and global instability of fluid-conveying pipes on elastic foundations", *J. Fluid. Struct.* **16**:1 (2002), 1–14.

[Elishakoff 2005] I. Elishakoff, "Controversy associated with the so-called "follower forces": critical overview", *Appl. Mech. Rev.* (*ASME*) **58**:2 (2005), 117–142.

[Elishakoff and Pellegrini 1987] I. Elishakoff and F. Pellegrini, "Exact and effective approximate solutions of some divergence-type non-conservative problems", *J. Sound Vib.* **114**:1 (1987), 143–147.

[de Langre et al. 2001] E. de Langre, O. Doaré, and F. Pellet, "Force suiveuse critique sur une colonne pesante semi-infinie: modèle et expériences", *Comptes Rendus de l'Académie des Sciences-Series IIB-Mechanics* **329**:3 (2001), 175–178.

[de Langre et al. 2007] E. de Langre, M. P. Païdoussis, O. Doaré, and Y. Modarres-Sadeghi, "Flutter of long flexible cylinders in axial flow", *J. Fluid Mech.* **571** (2007), 371–389.

[Langthjem and Sugiyama 2000] M. A. Langthjem and Y. Sugiyama, "Dynamic stability of columns subjected to follower loads: a survey", *J. Sound Vib.* **238**:5 (2000), 809–851.

[Lemaitre et al. 2005] C. Lemaitre, P. Hémon, and E. de Langre, "Instability of a long ribbon hanging in axial air flow", *J. Fluid. Struct.* **20**:7 (2005), 913–925.

[Naguleswaran 2004] S. Naguleswaran, "Transverse vibration of an uniform Euler–Bernoulli beam under linearly varying axial force", *J. Sound Vib.* **275**:1-2 (2004), 47–57.

[Obligado and Bourgoin 2013] M. Obligado and M. Bourgoin, "An experimental investigation of the equilibrium and stability of long towed cable systems", *New J. Phys.* **15**:4 (2013), 043019.

[Païdoussis 1998] M. P. Païdoussis, *Fluid-structure interactions: slender structures and axial flows, I*, Academic Press, San Diego, CA, 1998.

[Païdoussis 2003] M. P. Païdoussis, *Fluid-structure interactions: slender structures and axial flows, II*, Elsevier, San Diego, CA, 2003.

[Sugiyama and Kawagoe 1975] Y. Sugiyama and H. Kawagoe, "Vibration and stability of elastic columns under the combined action of uniformly distributed vertical and tangential forces", *J. Sound Vib.* **38**:3 (1975), 341–355.

[Triantafyllou and Chryssostomidis 1984] G. S. Triantafyllou and C. Chryssostomidis, "Analytic determination of the buckling speed of towed slender cylindrical beams", *J. Energy Resour. Technol.* (*ASME*) **106**:2 (1984), 246–249.

[Triantafyllou and Triantafyllou 1991] M. S. Triantafyllou and G. S. Triantafyllou, "The paradox of the hanging string: An explanation using singular perturbations", *J. Sound Vib.* **148**:2 (1991), 343–351.

Received 28 Dec 2013. Revised 3 Nov 2014. Accepted 25 Dec 2014.

EMMANUEL DE LANGRE: delangre@ladhyx.polytechnique.fr
Département de Mécanique, LadHyX, École Polytechnique, 91128 Palaiseau, France

OLIVIER DOARÉ: olivier.doare@ensta-paristech.fr
Unité de Mécanique, ENSTA-Paristech, 828 Boulevard des Maréchaux, 91120 Palaiseau, France

JOURNAL OF MECHANICS OF MATERIALS AND STRUCTURES

msp.org/jomms

Founded by Charles R. Steele and Marie-Louise Steele

See msp.org/jomms for submission guidelines.

JoMMS (ISSN 1559-3959) at Mathematical Sciences Publishers, 798 Evans Hall #6840, c/o University of California, Berkeley, CA 94720-3840, is published in 10 issues a year. The subscription price for 2015 is US $565/year for the electronic version, and $725/year (+$60, if shipping outside the US) for print and electronic. Subscriptions, requests for back issues, and changes of address should be sent to MSP.

JoMMS peer-review and production is managed by EditFLOW® from Mathematical Sciences Publishers.

PUBLISHED BY

mathematical sciences publishers

nonprofit scientific publishing

http://msp.org/

Journal of Mechanics of Materials and Structures

Volume 10, No. 3 May 2015

Special issue

In Memoriam: Huy Duong Bui

1559-3959(2015)10:3;1-A